Immobilization of *Mucor racemosus* NRRL 3631 lipase and characterization of silica-coated magnetite (Fe_3O_4) nanoparticles

Abeer A. El-Hadi[a,c], Hesham I. Saleh[b,d], Samia A. Moustafa[b] and Hanan M. Ahmed[a]

Departments of [a]Chemistry of Natural and Microbial Products, [b]Inorganic Chemistry, National Research Centre, Giza, Egypt, [c]Department of Biology, Faculty of Science, Taif University, Taif and [d]Department of Chemistry, Northern Border University, Arar, Saudi Arabia

Correspondence to Abeer A. El-Hadi, Department of Chemistry of Natural and Microbial Products, National Research Centre, El-Behoos St.33, Dokki, Giza 12311, Egypt
Tel: +20 233 54974; fax: +20 233 70931;
e-mail: abeerelhag67@yahoo.com

Received 29 July 2012
Accepted 1 October 2012

Egyptian Pharmaceutical Journal
2013,12:28–35

Introduction and purpose
The uncoated magnetite (M) and silica-coated magnetite (MS) nanoparticles have been suggested as carriers for the immobilization of enzymes to improve their activity and stability. The objective of this study was to demonstrate the potential use of magnetic nanoparticles in bioengineering applications, using *Mucor racemosus* NRRL 3631 lipase as the model enzyme.

Materials and methods
The magnetite (Fe_3O_4) particles were synthesized by the chemical coprecipitation technique, that is, Massart's process with minor modifications, using stable ferrous and ferric salts with ammonium hydroxide as the precipitating agent. The uncoated and coated magnetite nanoparticles for immobilizing the lipase were characterized according to the particle sizes, as measured from the transmission electron microscope images. The infrared and X-ray powder diffraction spectra can well explain the bonding interaction and crystal structures of various samples, respectively.

Results and conclusion
Different concentrations of silica-coated magnetite (MS) nanoparticles were used as cross-linking agents. A silica concentration of 1% was proven to be more suitable, with an immobilization efficiency of 96%. The transmission electron microscope images revealed the diameters of the uncoated magnetite particles to be 10–16 nm and those of the coated particles to be about 11 nm. The optimal pH and temperature of the immobilized lipase were 5–6 and 40°C, respectively. There was a slight decrease in the residual activity of the immobilized lipase at 60°C for 1 h. The kinetic constants V_{max} and K_m were determined to be 250 U/mg protein and 20 mmol/l, respectively, for the immobilized lipase. The residual activity of the immobilized lipase remained over 51% despite being used repeatedly seven times. It can be concluded that Fe_3O_4 magnetic nanoparticles and silica-coated magnetite (MS) nanoparticles have been successfully prepared with excellent properties using the chemical coprecipitation technique with some modifications. The silica coating appeared to be effective in protecting the magnetite from being converted to other oxide species. The results of the X-ray powder diffraction indicate that the composites were in the nanoscopic phase. The resulting immobilized lipase had better resistance to pH and temperature inactivation compared with free lipase and exhibited good reusability.

Keywords:
Fe_3O_4/SiO_2, immobilization efficiency, magnetic nanoparticles, *Mucor racemosus* NRRL 3631 lipase, stability

Egypt Pharm J 12:28–35

1687-4315

Introduction

In recent years, the use of nanophase materials offers many advantages because of their unique size and physical properties. Magnetic nanoparticles have become very popular when used in conjunction with biological materials such as proteins, peptides, enzymes, antibodies, and nucleic acids because of their unique properties [1]; this application is mainly based on the magnetic feature of the solid phase that helps in achieving a rapid and easy separation from the reaction medium in a magnetic field. Previous studies have reported that magnetic nanoparticles tend to lose their magnetizability when biopolymer-coated nanoparticles are circulated in the body [2]. Consequently, inorganic carrier materials including magnetite and silica gels were being focused on because of their thermal and mechanical stability, nontoxicity, and high resistance against microbial attacks and solutions of organic solvents [3]. Silica and its derivatives when coated onto the surface of magnetic nanoparticles may help to change their surface properties. With the appropriate coating, the magnetic dipolar attraction between the magnetic nanoparticles may be screened, thus minimizing or even preventing aggregation. The coating film could also provide a chemically inert layer against the nanoparticles, which is particularly

1687-4315 © 2013 Division of Pharmaceutical and Drug Industries Research, National Research Centre DOI: 10.7123/01.EPJ.0000427102.64865.32

useful in biological systems [1,4]. The larger specific surface area and surface reactive groups that are introduced by further modification of silica materials are favorable during the preparation of silica carriers for immobilized enzymes, and these carriers are very suitable for adsorption and immobilization of the adsorbed protein abundantly and steadily [5]. Lipases from different sources are currently used in enzymatic organic synthesis [6,7]. The expanding interest in lipases mainly lies on their wide industrial applications, including detergent formulation, oil/fat degradation, pharmaceutical synthesis, cosmetics, paper manufacture, and oleochemistry [8]. To use lipases more economically and efficiently in aqueous as well as in nonaqueous solvents, their activity and operational stability needs to be improved by immobilization. In addition, the enzyme immobilization onto magnetic supports such as nanosized magnetite particles allows an additional merit, namely, the selective and easy enzyme recovery from the medium under a magnetic force, compared with other conventional support materials. Hence, there is no need for expensive liquid chromatography systems, centrifuges, filters, or other equipment. In contrast, lipases obtain the highest activity when their molecules are immobilized onto nanoparticles because of their relatively high specific area; this promises results on immobilizing lipases onto surface-modified nano-sized magnetite particles [9].

The objective of this study was to demonstrate the potential use of magnetic nanoparticles in bioengineering applications. *Mucor racemosus* NRRL 3631 lipase was used as the model enzyme in this study. The uncoated and silica-coated magnetite nanoparticles were characterized by X-ray powder diffraction (XRD), transmission electron microscopy, and Fourier transform-infrared (IR) spectroscopy. The properties of the immobilized lipase such as activity, recovery, protein analysis, and thermal stability were investigated.

Materials and methods

Commercial lipase enzyme was prepared from *M. racemosus* NRRL 3631. All other materials were of analytical grade and used without further purification; these materials included tetraethyl orthosilicate (TEOS $\geq$ 98%), ammonia solution (NH_3, 28 wt%), ferrous dichloride tetrahydrate ($FeCl_2 \cdot 4H_2O$), ferric trichloride hexahydrate ($FeCl_3 \cdot 6H_2O$), glucose ($C_6H_6O_6$), potassium chloride (KCl), potassium dihydrogen phosphate (KH_2PO_4), magnesium sulfate ($MgSO_4 \cdot 7H_2O$), disodium hydrogen phosphate (Na_2HPO_4), sodium dihydrogen phosphate (NaH_2PO_4), peptone from animal protein, olive oil, gum arabic, and acetone.

Microorganisms, medium, and growth conditions

M. racemosus NRRL 3631 was maintained on potato dextrose agar (PDA) slants. The microorganism was grown in 250 ml Erlenmeyer flasks containing 100 ml of the medium. The medium was inoculated with 4 ml of spore suspension, and the flasks were incubated for 72 h in an orbital shaker operating at 200 rpm at 30°C. For lipase production, the composition of the basal medium (9% w/v) was: glucose, 1; olive oil, 1; peptone, 30; KH_2PO_4, 0.2; KCl, 0.05; and $MgSO_4 \cdot 7H_2O$, 0.05%, with an initial pH of 6.5 [10]. The medium was heat sterilized at 121°C for 15 min.

Standard method for enzyme activity assay

The lipase assay was performed using an olive oil emulsion according to the procedure described by Starr [11]. The olive oil emulsion was prepared as follows: 10 ml of olive oil and 90 ml of 10% arabic gum were emulsified using a homogenizer for 6 min at 20 000 rev/min. The reaction mixture composed of 3 ml of olive oil emulsion, 1 ml of 0.2 mol/l Tris-buffer (pH 7.5), 2.5 ml of distilled water, and 1 ml of enzyme solution was incubated at 37°C for 2 h with shaking. The emulsion was destroyed by the addition of 10 ml of acetone (95% v/v) immediately after incubation, and the liberated free fatty acids were titrated with 0.05 N.

Analytical procedure of protein determination

Protein measurements were carried out according to the method of Lowry *et al.* [12], using BSA as the standard. The amount of bound protein was determined indirectly from the difference between the amount of protein present in the filtrate and that in washing solutions after immobilization.

Partial purification of *M. racemosus* lipase using ammonium sulfate

Ammonium sulfate (60% saturation) was added to 900 ml of the culture supernatant at 4°C. The precipitate was collected by centrifugation at 12 000*g* at 4°C for 20 min and dissolved in a constant amount of distilled water. The lipase activity and protein concentrations were determined [13].

Synthesis of magnetite nanoparticles

The nanoparticles were prepared according to the method described by Massart [14] but without the use of hydrochloric acid. A total of 4.05 g of $FeCl_3 \cdot 6H_2O$ and 1.98 g of $FeCl_2 \cdot 4H_2O$ was dissolved in 100 ml of distilled water; the solution was purged with nitrogen to agitate the mixture and prevent the oxidation of Fe^{2+} ions. After 30 min of purging, 143 ml of 0.7 mol/l NH_4OH was added dropwise into the solution and the now basified solution was purged for an additional 10 min. During the addition of NH_4OH, it was noticed that the solution changed color from the original brown to dark brown and then to black. The precipitate was magnetically separated using a permanent magnet and then washed with distilled water several times and allowed to dry in air. The resulting product was defined as M.

Synthesis of silica-coated magnetite nanoparticles

The above-mentioned experiment was repeated until the step in which the solution was purged with nitrogen to agitate the mixture. After this step, the precursor TEOS (3 ml) was carefully dropped into the reaction mixture of iron using a syringe, with mechanical stirring.

The homogenization was performed for 15 min. After sonication for 15 min, 143 ml of 0.7 mol/l NH_4OH was added dropwise into the mixture with continuous mechanical stirring for 30 min. The coated particles were finally separated from the liquid using a permanent magnet, washed with distilled water several times, and allowed to dry in air. Finally, we also determined the effect of silica coating by varying the amount of TEOS added to the reaction mixture. In this regard, we studied the effect of five different amounts of TEOS, 1.04, 2.08, 4.22, 8.33, and 12.5 ml, which are equivalent to 0.5, 1, 2, 4, and 6% molar ratios, respectively. The determine parameter of silica-coated magnetite nanoparticles is labeled as MS1, MS2, MS3, MS4 and MS5.

Characterization

XRD was used to investigate the crystal structure of the magnetic nanoparticles. The size and shape of the nanoparticles were examined using a transmission electron microscope (TEM) (Model JEOL-1230, Japan). The IR spectra were recorded using a Fourier transform-infrared spectrophotometer (FT-IR). The sample and KBr were pressed to form a tablet.

Immobilization of lipase

Because of the epoxy groups of the magnetite silica nanoparticles, lipase immobilization was carried out by treatment of the lipase solution with the nanoparticles directly. The particles (200 mg of Fe_3O_4 coated with 1% silica nanoparticles) were added to 40 ml of phosphate buffer (0.1 mol/l, pH 6.5) containing lipase (1 ml). The mixture was placed in a shaking incubator at 30°C with continuous shaking at 150 rpm for 6 h to finish the immobilization of lipase. The immobilized lipase was recovered by magnetic separation and washed with phosphate buffer (0.1 mol/l, pH 6.5) three times to remove excess enzyme. The resulting immobilized lipase was held at 4°C before use. The enzymatic activities of the free and immobilized lipases were measured by titrating the fatty acids that were obtained from the hydrolysis of olive oil. One unit of lipase activity (U) is defined as the amount of enzyme that hydrolyzes olive oil, liberating 1.0 μmol of fatty acid per minute under the assay conditions. The relative recovery (%) was the ratio between the activity of the immobilized lipase and that of free lipase [15].

Biochemical characterization of the free and immobilized lipases and their reusability

Thermal stability of the free and immobilized lipase was studied by incubating the biocatalyst at 30–80°C for 15, 30, and 60 min in a water bath. Similarly, to determine the stability at varying pH values, the immobilized enzyme was reinsulated separately in 0.2 mol/l of citrate buffer at pH 3–7 and in tris-HCl buffer at pH 7.6–9 for 1 h, and the residual activities were determined under standard assay conditions. The residual activity in the samples without incubation was considered to be 100%. The inactivation rate constant (K) and the half-life time ($t_{1/2}$) were calculated using the following formula: Half-life = 0.693/K, in which K is the deactivation rate constant = slope of the straight line [16].

The kinetic parameters V_{max} and K_m were determined for the immobilized lipase. In addition, the reusability of the immobilized lipase was determined by hydrolysis of olive oil by the immobilized lipase recovered using magnetic separation and compared with the first run (activity defined as 100%).

Results and discussion

Structure and shape of the support for nanoparticles

The XRD pattern (Fig. 1) of the Fe_3O_4 (M) nanoparticles prepared under standard conditions revealed diffraction peaks at 111, 220, 311, 400, 422, 511, 440, etc., which were the characteristic peaks of Fe_3O_4 crystals with a cubic spinel structure [17]. It was clear that only the phases of Fe_3O_4 were detectable and there were no other undesired diffraction maximas of the impurities that could be observed in the spectra. From the relatively wide half-peak breadth, it could be estimated that the particle size is quite small. From the XRD patterns, the average diameter that was calculated to be 13.8 nm using the Scherrer equation ($D = K\lambda/\beta \cos\theta$, in which K is constant, λ is X-ray wavelength, and β is the peak width of half-maximum) [18,19]. Interestingly, it was observed that the diffraction patterns for the samples MS1 and MS2

Figure 1

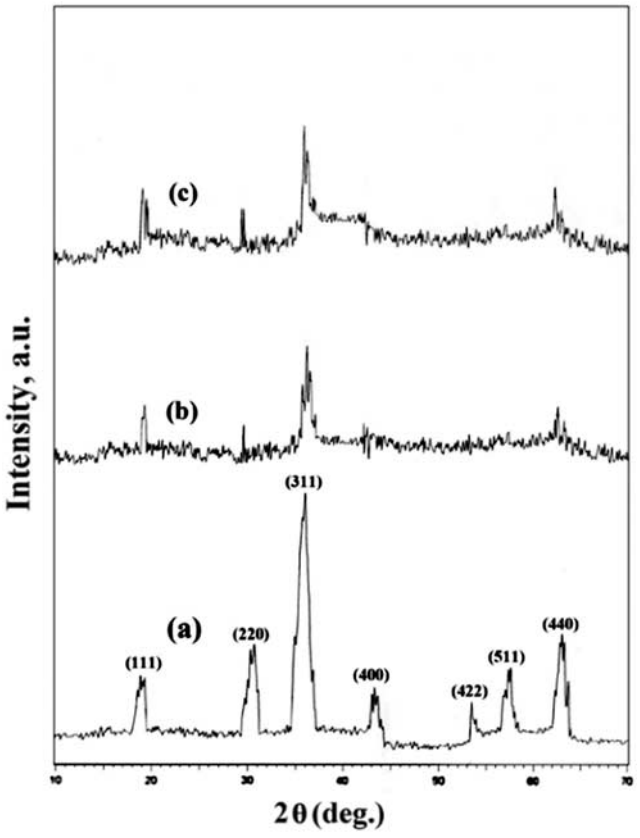

X-ray powder diffraction patterns of (a) pure Fe_3O_4 nanoparticles and (b) MS1 and MS2.

consisted of an amorphous structure, which was attributed to the amorphous silica matrix, as clearly indicated in Fig. 1 [20]. The XRD patterns of the remaining samples MS3, MS4, and MS5 (not presented here) also showed an amorphous structure. The relatively low intensity reflections and absence of significant sharp diffraction peaks for the MS1 and MS2 patterns are probably due to the presence of SiO_2 on the surface of the magnetic nanoparticles. Xu *et al.* [21] also suggested that the low intensity of the reflection peaks could be attributed to the ultrafine crystalline structure of the magnetite particles used for the generation of silica-coated nanoparticles. The particle size and morphology of Fe_3O_4, Fe_3O_4/SiO_2, and Fe_3O_4/SiO_2/enzyme were evaluated from the TEM micrographs. It is noteworthy that the size distribution is 10–16 nm, which matched the value calculated using the Scherrer equation, and that the nanoparticles are spherical in shape (Fig. 2a) and their aggregation can be discerned clearly. In Fig. 2b and c, the coated silica layer can be observed as a typical core–shell structure of the Fe_3O_4/SiO_2 nanoparticles. The dispersity of the Fe_3O_4/SiO_2 nanoparticles was also improved, and the average size increased to about 32 nm. After lipase adsorption, the degree of particle aggregation increased; however, a change in the particle size was not observed (Fig. 2d).

FT-IR spectra of the magnetite nanoparticles

The FT-IR spectra of magnetite are shown in Fig. 3. A factor group analysis, reported in a classic IR study on spinels, suggested that there were four IR-active bands; however, in most cases, including magnetite, only two of them are observed between 400 and 800 cm^{-1} [22]. In this study, Fe_3O_4 showed a broad band that consisted of two slightly split peaks identified at 573 and 621 cm^{-1}; these peaks were attributed to the stretching vibration of

Figure 2

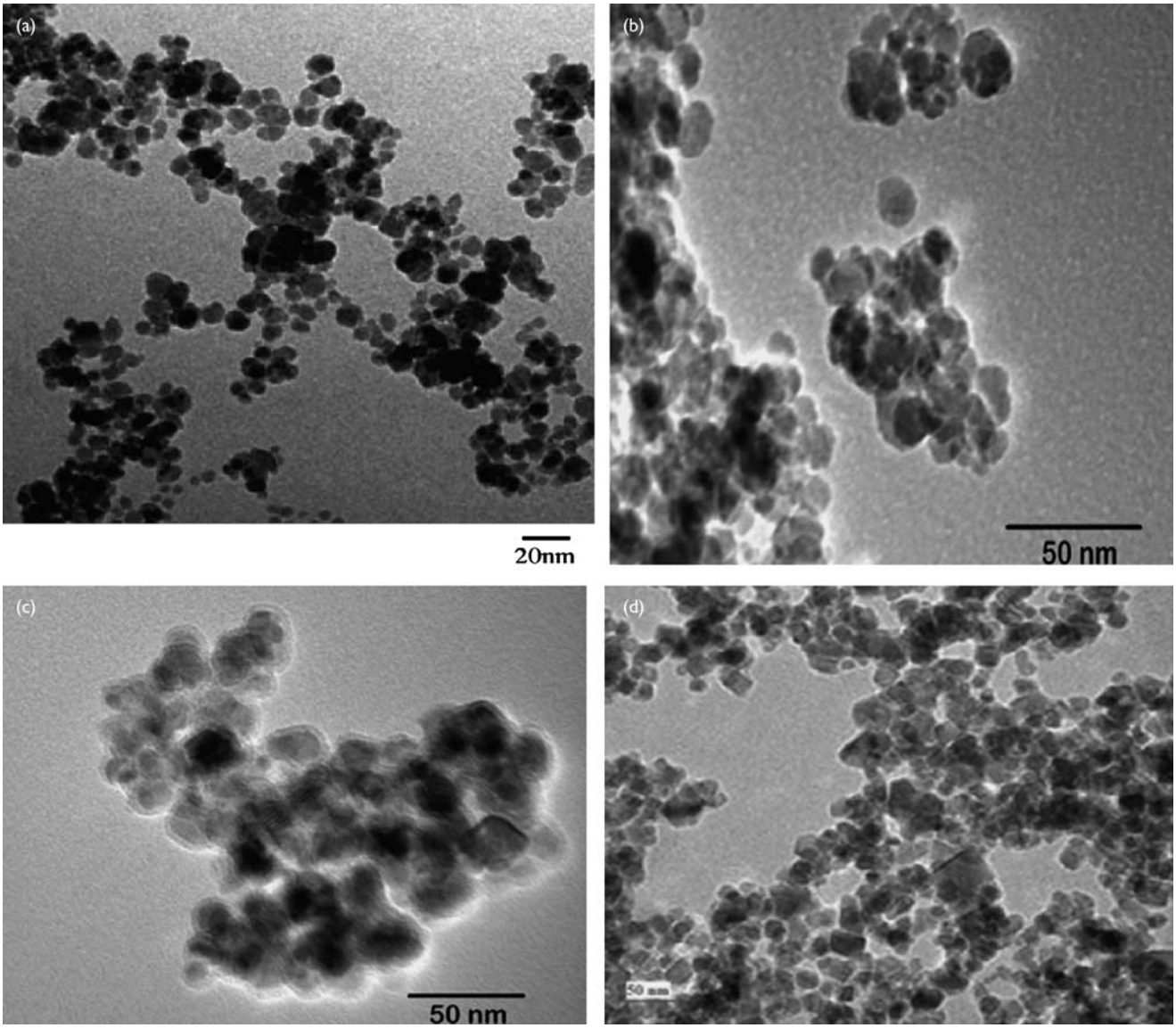

Transmission electron microscope images of (a) Fe_3O_4 nanoparticles, (b) MS1 nanoparticles, (c) MS1 nanoparticles with immobilized lipase, and (d) MS1 nanoparticles without lipase.

the Fe–O bond and confirmed the occupancy of Fe^{3+} ions at tetrahedral sites in a manner consistent with that reported in the literature [23–25]. On the low-frequency side of the broad band, we observed that the weak peaks appearing at 432 and 453 cm^{-1} corresponded to the presence of the Fe^{3+}–O^{2-} bond at octahedral sites [26]. In contrast, we found a broad peak near 3380 cm^{-1} and a sharp peak near 1635 cm^{-1}, which were attributed to the stretching and binding vibrations of the hydroxyl groups. These peaks confirm the presence of adsorbed water on the surface of magnetite [27]. However, the peaks at 1383 and 1453 cm^{-1} resulted from the stretching vibration of the C–O bonds in CO_2, which might come from air.

FT-IR spectra of the silica-coated magnetite nanoparticles

Figure 3 shows the IR spectrum of the silica-coated magnetite nanoparticles. It was clear that the characteristic adsorption bands of the Fe–O bond (Fe^{3+}–O^{2-}) of the silica-coated magnetite nanoparticles shift to higher wave numbers of 585, 637, 441, and 483 cm^{-1}, respectively, compared with that of uncoated nanoparticles (in 573, 621, 432, and 453 cm^{-1}). The absorption bands at around 1030, 800, and 470 cm^{-1} reflect the Si–O–Si asymmetry, Si–O–Si symmetric stretching vibrations, and deformation mode of Si–O–Si, respectively [28]. The bands at 569 and 965 cm^{-1} are possibly because of the Fe–O–Si and Si–O–Si stretching vibrations caused by the perturbation of the metallic ion in the SiO_4 tetrahedra [29], respectively. The FT-IR spectra of the lipase on the silica-coated magnetite nanoparticles (Fig. 3) showed a spectra similar to the IR spectra of the silica-coated magnetite nanoparticles with immobilized lipase. It was observed that the characteristic bands of lipase at 1655 and 1535 cm^{-1} [30] revealed that it was immobilized on the silica-coated magnetite nanoparticles.

Figure 3

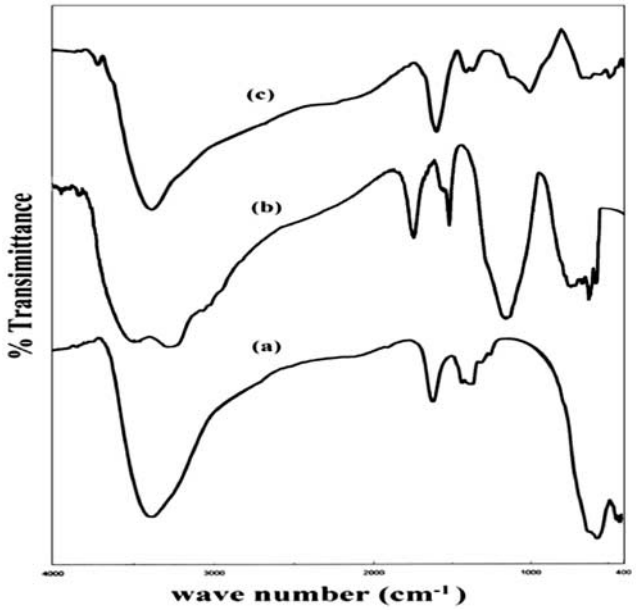

(a) Fourier transform-infrared spectrophotometer spectra of Fe_3O_4, (b) MSI without immobilized lipase, and (c) MSI with immobilized lipase.

The amount of enzyme added and the corresponding immobilization efficiency

The relationship between the amounts of enzyme (0.5–3 ml) and immobilization efficiency has been shown in Fig. 4. When the enzyme amount added was 1 and 1.5 ml, with 300 mg of the magnetite coated with 1% silica, the maximal immobilization efficiency was 87 and 96%, respectively. The curve in Fig. 4 illustrates that the immobilization efficiency gradually decreases when the amount of enzyme added is more than 1.5 ml. This could be explained by an overall amount of the added enzyme formed an intermolecular space hindrance of the immobilized enzyme, which will not only the active site of the enzymes but also restrain the dispersion of the substrate and product [3].

Effect of different concentrations of SiO_2 coating the magnetite nanoparticles on the immobilization efficiency of lipase

To solve the leaching problems of the adsorbed lipase and improve the conventional way for lipase immobilization, different concentrations of MS nanoparticles ranging from 0.5–4% were used as cross-linking agents for immobilization in 300 mg of magnetite nanoparticles. The experimental results have been given in Fig. 5. It was shown that the immobilization efficiency decreased slightly from 96 to 84% with an increase in the SiO_2 concentration from 1 to 4% and then decreased sharply with a further increase in the concentration of SiO_2 to 6% (76%). Although a higher amount of lipase binding occurred when a low concentration of SiO_2 was used for silica coating the magnetic nanoparticles, there was a substantial loss of enzyme activity.

Biochemical properties of the free and immobilized lipase

The effect of pH on the specific enzyme activity of lipase immobilized by silica was studied by varying the pH of the reaction medium from 3–9 using a 0.1 mol/l citrate phosphate buffer (3–7) and a 0.1 mol/l Tris (hydroxy

Figure 4

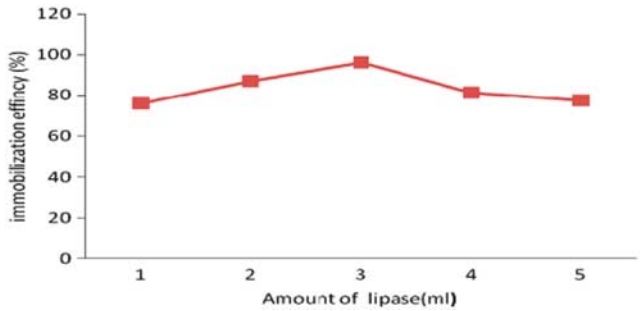

Effect of different amounts of *Mucor racemosus* NRRL 3631 lipase on the immobilization efficiency.

methyl) amino methane buffer (7.5–9), and the pH profile has been shown in Fig. 6a. Generally, the binding of enzymes to polycationic supports would result in an acidic shift in the optimum pH [31,30]; similarly, after silica immobilization, the optimum pH of lipase exhibited an acidic shift (5–6). The variation in the residual activity of the free and immobilized lipase with pH is shown in Fig. 6b. The immobilized lipase was stable in the pH range of 3–5 as compared with the free enzyme; this indicated that immobilization appreciably improved the stability of lipase in the acidic region.

The thermal stabilities of the free and immobilized lipase in terms of the residual activities have been compared in Fig. 7. Lipase immobilized on MS nanoparticles remained fully active up to 40°C. These results are similar to those obtained by Huang *et al.* [30], who found that binary immobilized lipase from *Candida rugosa* was fully active at 40°C; however, inactivation of the enzyme occurred on treatment at higher temperatures. About 40% of the residual activity of free lipase was preserved at 60°C for 1 h; however, about 72.9% residual activity was preserved in case of the immobilized enzyme. At 80°C, the free enzyme was fully inactivated, whereas the immobilized form preserved about 37.8% of its residual activity for 15 min. Hiol *et al.* [32] studied the thermostability of the free enzyme of *Rhizopus oryzae* and found that it was highly inactivated at 45°C and almost all activity was lost at 50°C after a 40 min incubation. This thermal stabilization could be explained by the location of the lipase inside the micropores of the support, wherein the enzyme is protected against alterations of the microenvironment. The Michaelis–Menten kinetics of the hydrolytic activity of the free and immobilized lipases have been represented in Table 1, using varying initial concentrations of olive oil as the substrate. The Michaelis constant (K_m) and the maximum reaction velocity (V_{max}) were evaluated from the double reciprocal plot. The V_{max} value of 250 U/mg protein exhibited by the immobilized lipase was found to be higher than that of free lipase (50 U/mg protein). The K_m value (20 mmol/l) determined for the immobilized lipase was about three-folds higher than that of free lipase (6.66 mmol/l), which indicated a lower affinity toward the substrate. This increase in K_m might be either due to the structural changes induced in the enzymes by the immobilization or the lower accessibility of the substrate to the active sites [33,30]. The inactivation temperature of the soluble and immobilized lipase was observed to be between 50 and 70°C. In general, the immobilization processes protected the enzymes against heat inactivation, for example, the calculated half-life values at 50, 60, and 70°C for the immobilized enzyme were 630, 533, and 391.5 min, respectively, which are higher than those (231, 198, 187, and 3 min, respectively) of the free enzyme as shown in Table 2, that is, the free enzyme showed a half-life of 10.5 h at 50°C, 8.88 h at 60°, and 6.5 h at 70°C. Our results are nearly similar to those obtained by Kumar *et al.* [34], who reported the half-life of *Bacillus coagulans* BTS_3 lipase at 55 and 60°C to be 2 h and 30 min, respectively; moreover, they reported the half-life of lipase from another mesophilic bacteria (*Bacillus* spp.) to be 2 h at 60°C. They reported that the deactivation rate constants of 1.1×10^{-3}, 1.3×10^{-3}, and 1.7×10^{-3} for the experimental immobilized enzyme at temperatures of 50,60, and 70°C, respectively were lower than those (3×10^{-3}, 3.77×10^{-3},

Figure 5

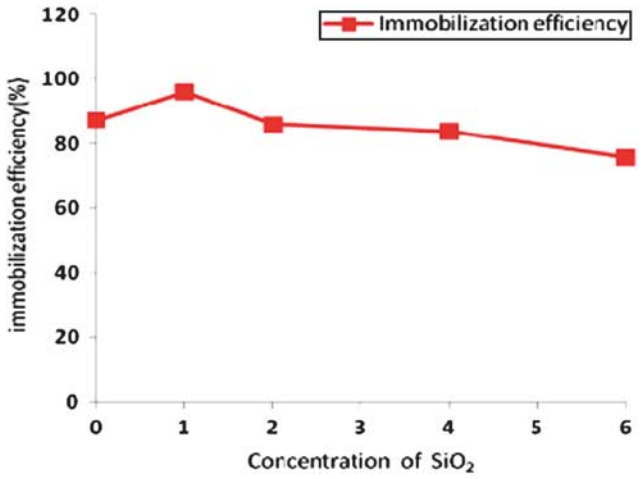

Effect of different concentration of SiO_2-coated magnetic nanoparticles on the immobilization efficiency of *Mucor racemosus* NRRL 3631 lipase.

Figure 6

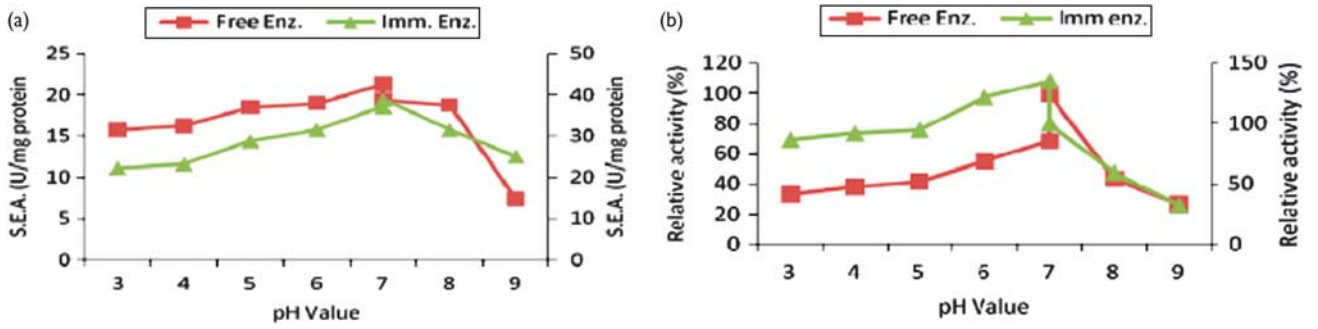

Effect of pH values on the activity (a) and stability (b) of free and immobilized *Mucor racemosus* lipases.

Figure 7

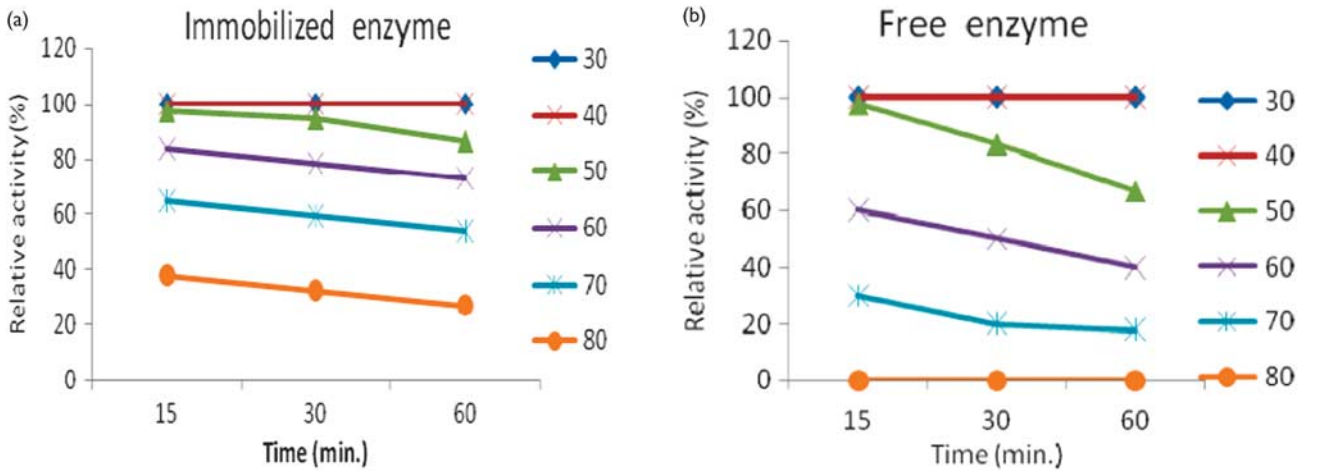

Thermal stability of free and immobilized *Mucor racemosus* NRRL 3631 lipases.

Table 1 Kinetic parameters (V_{max} and K_m) for the free and immobilized enzymes

Types	V_{max} (U/mg protein)	K_m (mmol/l)
Immobilized lipase	250	20
Free lipase	50	6.66

Table 2 Kinetic parameters (half-life and the deactivation rate constant) for the free and immobilized enzymes

	Half-life (min)			Deactivation rate constant		
Types	50°C	60°C	70°C	50°C	60°C	70°C
Immobilized lipase	630	533	391.5	1.8×10^{-3}	1.3×10^{-3}	1.7×10^{-3}
Free lipase	231	198	187.3	3×10^{-3}	3.77×10^{-3}	4.8×10^{-3}

Figure 8

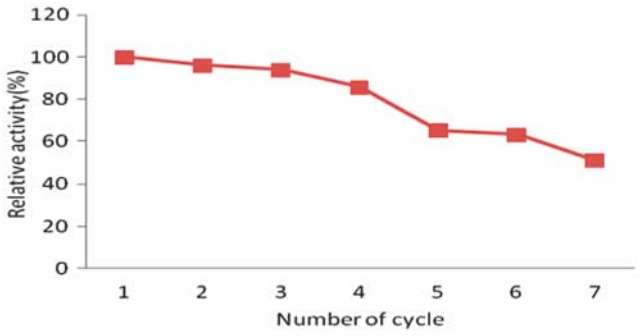

Operational stability of the immobilized *Mucor racemosus* NRRL lipase on the hydrolysis process.

and 4.8×10^{-3}, respectively) of the free enzyme at the same temperatures. These results could be related to a hydrophilic or hydrophobic environment. A hydrophilic microenvironment allowed the immobilized derivatives to follow a double experimental decay in their activities, wherein the hydrophobic microenvironment makes the enzymatic activity suffer a single experimental decay during storage conditions [35].

Variations in the enzyme activity with repeated batch enzyme reactions

Operational stability was the most important parameter in the immobilization of enzymes because inactivation is inevitable when the free enzyme is exposed to inadequate ambient conditions. The recycling efficiency of the immobilized lipase has been presented in Fig. 8. It was observed that the immobilized lipase retained 51% of its original activity even after the seventh reuse; this indicated that the resultant bound lipase had a better reusability, which was desirable for applications in biotechnology. The loss of activity may be ascribed to conformational changes in the enzyme, blocking of the lipase active sites, or the gradual loss of the bound lipase during the reaction procedures.

Conclusion

From these results it can be concluded that Fe_3O_4 magnetic nanoparticles and silica-coated magnetite (MS) nanoparticles with excellent properties have been successfully prepared using the chemical coprecipitation technique with some modifications. The XRD results indicate that the composites were in the nanoscopic phase. Based on the TEM images, the diameters of the uncoated magnetite particles were determined to be around 10–16 nm and those of the coated particles to be about 11 nm. The silica coating appeared to be effective in protecting the magnetite from being converted to other oxide species. The thermal and pH stabilities of the immobilized lipase increased on immobilization. The optimal pH and temperature of the immobilized lipase were 5–6 and 40°C, respectively. There was a slight decrease in the residual activity of the immobilized lipase. The operational stability of the immobilized lipase

over repeated cycles could substantially save on the cost of the enzyme. The residual activity of the enzyme even after seven repeated uses was over 51%. Conclusively, magnetic nanoparticles provide an economically efficient and selective system for enzyme immobilization.

Acknowledgements

Conflicts of interest

There are no conflicts of interest.

References

1 Lei L, Liu X, Li Y, Cui Y, Yang Y, Qin G. Study on synthesis of poly(GMA)-grafted Fe_3O_4/SiO X magnetic nanoparticles using atom transfer radical polymerization and their application for lipase immobilization. Mater Chem Phys 2011; 125:866–871.

2 Duguet E, Vasseur S, Mornet S, Goglio G, Demourgues A, Portier J, *et al.* Towards a versatile platform based on magnetic nanoparticles for in vivo applications. Bull Mater Sci 2006; 29:581–586.

3 Bai Y-X, Li Y-F, Yang Y, Yi L-X. Covalent immobilization of triacylglycerol lipase onto functionalized novel mesoporous silica supports. J Biotechnol 2006; 125:574–582.

4 Deng Y-H, Wang C-C, Hu J-H, Yang W-L, Fu S-K. Investigation of formation of silica-coated magnetite nanoparticles via sol-gel approach. Colloids and Surfaces A: Physicochem Eng Aspects 2005; 262 (1–3):87–93.

5 Park D, Haam S, Jang K, Ahn IS, Kim WS. Immobilization of starch-converting enzymes on surface-modified carriers using single and co-immobilized systems: properties and application to starch hydrolysis. Process Biochem 2005; 40:53–61.

6 Yu H, Ching CB. Theoretical analysis of the adsorption effect on kinetic resolution of racemates catalyzed by immobilized enzymes in a batch reactor. Ind Eng Chem Res 2008; 47:4251–4255.

7 Villeneuve P, Muderhaw JM, Graille J, Haas MJJ. Lipase-catalyzed esterification of Betulinic acid using phthalic anhydrid in organic solvent media: study of reaction parameters. Mol Catal B Enzyme 2000; 9:113–148.

8 Mostafa H, El-Hadi AA. Immobilization of *Mucor racemosus* NRRL 3631 lipase with different polymer carriers produced by radiation polymerization. Mal J Microb 2010; 6:149–155.

9 Lee SH, Doan TTN, Won K, Ha SH, Koo Y-M. Immobilization of lipase within carbon nanotube-silica composites for non-aqueous reaction systems. J Mol Catal B: Enzymatic 2010; 62:169–172.

10 Akhtar MW, Mirza AQ, Chughtai MID. Lipase induction in *Mucor hiemalis.* Appl Environ Microbiol 1980; 40:257–263.

11 Starr MP. Spirit blue agar: a medium for the detection of lipolytic microorganisms. Science 1941; 93:333–334.

12 Lowry OH, Rosebrough NJ, Farr AL, Randall RJ. Protein measurement with the Folin phenol reagent. J Biol Chem 1951; 193:265–275.

13 Abbas H, Hiol A, Deyris V, Comeau L. Isolation and characterization of an extracellular lipase from *Mucor* sp. strain isolated from palm fruit. Enzyme Microb Technol 2002; 31:968–975.

14 Massart R. Preparation of aqueous magnetic liquids in alkaline and acidic media. IEEE Trans Magnetics 1981; 17:1247–1248.

15 Lee DH, Park CH, Yeo JM, Kim SW. Lipase immobilization on silica gel using a cross-linking method. J Ind Eng Chem 2006; 12:777–782.

16 Bailey JE, Ollis DF. *Biochemical engineering fundamentals*. 2nd ed. USA: Mc Graw-Hill Book Company; 1986.

17 Nedkov I, Kolev S, Zadro K, Krezhov K, Merodiiska T. Crystalline anisotropy and cation distribution in nanosized quasi-spherical ferroxide particles. J Magn Magn Mater 2004; 272–276 (Suppl 1):e1175–e1176.

18 Warren BE. *X-ray diffraction*. New York: Dover publications; 1990.

19 Hong YR, Li HJ, Zhang ZS, Li ZH, Zheng Y, Ding MJ, Wei GD. Preparation and characterization of silica-coated Fe_3O_4 nanoparticles used as precursor of ferrofluids. App Surf Sci 2006; 255:3485–3492.

20 Poulsen HF, Neuefeind J, Neumann H-B, Schneider JR, Zeidler MD. Amorphous silica studied by high energy X-ray diffraction. J Non-Cryst Sol 1995; 188 (1–2):63–74.

21 Xu H, Tong N, Cui L, Lu Y, Gu H. Preparation of hydrophilic magnetic nanospheres with high saturation magnetization. J Magn Magn Mater 2007; 311 (Special Issue):125–130.

22 White WB, DeAngelis BA. Interpretation of the vibrational spectra of spinels. Spectrochim Acta A Mol Spectrosc 1967; 23:985–995.

23 Ma M, Zhang Y, Yu W, Shen H-Y, Zhang H, Gu N. Preparation and characterization of magnetite nanoparticles coated by amino silane. Colloids and Surfaces A: Physicochem Eng Aspects 2003; 212:219–226.

24 Guang-She L, Li-Ping L, Smith RL Jr, Inomata H. Characterization of the dispersion process for $NiFe_2O_4$ nanocrystals in a silica matrix with infrared spectroscopy and electron paramagnetic resonance. J Mol Struct 2001; 560 (1–3):87–93.

25 Li Y-S, Church JS, Woodhead AL, Moussa F. Preparation and characterization of silica coated iron oxide magnetic nano-particles. Spectrochim Acta A Mol Biomol Spectrosc 2010; 76:484–489.

26 Maity D, Agrawal DC. Synthesis of iron oxide nanoparticles under oxidizing environment and their stabilization in aqueous and non-aqueous media. J Magn Magn Mater 2007; 308:46–55.

27 Tie S-L, Lin Y-Q, Lee H-C, Bae Y-S, Lee C-H. Amino acid-coated nano-sized magnetite particles prepared by two-step transformation. Colloids and Surfaces A: Physicochem Eng Aspects 2006; 273 (1–3):75–83.

28 Arruebo M, Fernández-Pacheco R, Irusta S, Arbiol J, Ibarra MR, Santamaría J. Sustained release of doxorubicin from zeolite-magnetite nanocomposites prepared by mechanical activation. Nanotechnology 2006; 17: 4057–4064.

29 Chang C-F, Lin P-H, Höll W. Aluminum-type superparamagnetic adsorbents: synthesis and application on fluoride removal. Colloids and Surfaces A: Physicochem Eng Aspects 2006; 280 (1–3):194–202.

30 Huang S-H, Liao M-H, Chen D-H. Direct binding and characterization of lipase onto magnetic nanoparticles. Biotechnol Prog 2003; 19:1095–1100.

31 Goldstein L, Levin Y, Katchalski E. A water-insoluble polyanionic derivative of trypsin. II. Effect of the polyelectrolyte carrier on the kinetic behavior of the bound trypsin. Biochemistry 1965; 3:1913–1919.

32 Hiol A, Jonzo MD, Rugani N, Druet D, Sarda L, Comeau LC. Purification and characterization of an extracellular lipase from a thermophilic *Rhizopus oryzae* strain isolated from palm fruit. Enzyme Microb Technol 2000; 26 (5–6):421–430.

33 Anita A, Sastry CA, Hashim MA. Immobilization of urease on vermiculite. Bioprocess Eng 1997; 16:375–380.

34 Kumar S, Kikon K, Upadhyay A, Kanwar SS, Gupta R. Production, purification, and characterization of lipase from thermophilic and alkaliphilic *Bacillus coagulans* BTS-3. Protein Expr Purif 2005; 41:38–44.

35 Moreno JM, Arroyo M, Hernáiz M-J, Sinisterra JV. Covalent immobilization of pure isoenzymes from lipase of *Candida rugosa.* Enzyme Microb Technol 1997; 21:552–558.